Sensors & Actuators: B. Chemical 334 (2021) 129664

Contents lists available at ScienceDirect

Sensors and Actuators: B. Chemical

journal homepage: www.elsevier.com/locate/snb

Measurement of respiration and acidification rates of mammalian cells in thermoplastic microfluidic devices

Bernhard Müller [a], Philipp Sulzer [a], Manuel Walch [b], Helene Zirath [c], Tomáš Buryška [d,1], Mario Rothbauer [c], Peter Ertl [c], Torsten Mayr [a,*]

[a] Institute of Analytical Chemistry and Food Chemistry, Graz University of Technology, Stremayrgasse 9, 8010, Graz, Austria
[b] Kdg Opticomp GmbH, Am kdg Campus, Dorf 91, 6652, Elbigenalp, Austria
[c] Institute of Applied Synthetic Chemistry, Vienna University of Technology, Getreidemarkt 9/163, 1060, Vienna, Austria
[d] Loschmidt Laboratories, Department of Experimental Biology and RECETOX, Faculty of Science, Masaryk University, Kamenice 5, Brno, 625 00, Czech Republic

ARTICLE INFO

Keywords:
Luminescent optical sensor
Oxygen pO2
pH
Online-monitoring
Perfused cell culture
Metabolism

ABSTRACT

Luminescent chemical sensors have been proven to be a valuable asset in cell cultures and generally in microbiological studies. We present microfluidic cell culture devices with integrated optical chemical sensors. The integrated sensors offer the possibility to monitor dissolved oxygen and pH levels and enable the measurement of respiration and acidification rates. The cell metabolism was observed using this method by temporarily stopping the incubation flow, barely influencing the cell culture. A thermoplastic polymer is used as oxygen impermeable chip material to enable the measurement of respiration rates, which is not possible with widely used PDMS-based microfluidics. Hence, an innovative fast prototyping strategy is utilized to enable the replication of small series of thermoplastic microfluidic chips. We were able to demonstrate the suitability of this measurement method by monitoring the metabolic response of a human lung carcinoma epithelial-like cell line (A549) to the exposure of FCCP (Carbonyl cyanide-4-(trifluoromethoxy)phenylhydrazone), a drug known for its up-regulating effect on respiration and acidification rates. This universal measurement approach can potentially be deployed in all sorts of microfluidic devices and help to retrieve valuable data from inside those systems beyond classical end-point detection methods. It therefore complements modern 3D cell cultures and organ-on-chip research with a powerful analytical technology for gathering information about ongoing cell metabolism.

1. Introduction

The past decade has seen the rapid development of microfluidic technology in different fields, ranging from lab-on-a-chip applications to organ-on-chip technology. To fully take advantage of the controlled and well-defined microfluidic environment, sensor integration into those systems is essential [1]. To date, mainly end-point detection methods, like cell viability assays, are available which only allow characterization of highly toxic compounds causing permanent cellular changes [2]. Gathering real-time information from inside microfluidic chips is therefore crucial for the evaluation of metabolism and functional parameters. This task has proven to be challenging and only limited technologies exist, especially with regards to parallelization and multi-parameter read-out. Moreover, most microfluidic devices are designed as a single use platform and therefore cost-efficient sensors are essential for a wider use.

One common method to gather information from living cell tissue is the measurement of the activity of muscle tissues by observing the bending of flexible pillars. This method does not only measure present forces, but can also evaluate cardiac beat dynamics via pixel analysis of image data as assessment for cardiac health, instead of classical cell viability [3–5]. Another method is the utilization of microelectrode

Abbreviations: FCCP, Carbonyl cyanide-4-(trifluoromethoxy)phenylhydrazone; COC, cyclic olefin copolymer; OHC12, 4-(5,5-difluoro-7-(4-hydroxyphenyl)-1,9-diphenyl-5H-5λ4,6λ4-dipyrrolo[1,2-c2′,1′-f][1,3,5,2]triazaborinin-3-yl)-N-dodecylbenzamide; ptBS particles, Poly-tert-butylstyrene particles; PtTPTBPF, platinum (II)-meso-tetra(4-fluorophenyl)tetrabenzoporphyrin; POF, polymer optical fiber.

* Corresponding author at: Torsten Mayr – Graz University of Technology, Institute for Analytical Chemistry and Food Chemistry, Austria.
E-mail addresses: bernhhrd.mueller@tugraz.at (B. Müller), philipp.sulzer@gmx.at (P. Sulzer), office@kdg.at (M. Walch), helene.zirath@tuwien.ac.at (H. Zirath), tomas.buryska@chem.ethz.ch (T. Buryška), mario.rothbauer@tuwien.ac.at (M. Rothbauer), peter.ertl@tuwien.ac.at (P. Ertl), torsten.mayr@tugraz.at (T. Mayr).
[1] Present Addresses: Institute for Chemical and Bioengineering, ETH Zürich, Vladimir Prelog Weg 1, 8093 Zürich, Switzerland.

https://doi.org/10.1016/j.snb.2021.129664
Received 15 October 2020; Received in revised form 29 January 2021; Accepted 10 February 2021
Available online 16 February 2021

arrays (MEAs) to assess electrophysiological dynamics of neuronal and cardiac tissues [3,6–8]. The integrity of barrier tissues, like the blood brain barrier, gastrointestinal tract and skin, can be investigated with a similar technique noninvasively via transepithelial/endothelial electrical resistance (TEER) measurements [9–12].

Integration of electrochemical sensors has been utilized for monitoring external parameters in microfluidic systems. For example, detection of dissolved oxygen has been shown with miniaturized electrodes, implemented via inkjet printing technique [13]. Further parameters, like pH [14] and temperature [2], have also been realized as electrochemical sensors. There have also been huge advances in the development of electrochemical immune-biosensors for monitoring soluble biomarkers in recent years [15,16]. In general, those electrochemical sensors are difficult to integrate, require a reference electrode and in some cases even consume the analyte.

However, this is not the case for optical detection methods and luminescent optical sensors have proven to be a good approach since they are easy to miniaturize, can be read out externally and can be produced at a low cost. Optical oxygen measurements have been successfully integrated in various applications reaching from microbioreactors to cell cultures in static chambers or microfluidic devices [17–22]. Even a pesticide detection module, based on the respiration of algae, has been realized [23]. Luminescent pH measurements are more difficult, due to a lack of stable and bright pH indicators, and are so far mainly done via absorption measurements of phenol red present in the incubation media [2]. However, absorption measurements of the media are intrinsically difficult to scale down to small channel heights for true microfluidic systems since a certain pathlength is required to gain distinguishable signal changes.

The possibility of monitoring these extrinsic parameters is already a huge progress in terms of reliable cell conditioning and understanding cell activity. However, it still does not enable analysis of cell metabolism and only to a certain extent examination of non-lethal effects of potentially toxic substances. In this regard, the measurement of respiration and acidification rates is a much more powerful tool, since those measurements lead to a better understanding of the ongoing cell metabolism. Papkovsky and Dmitriev [24] have summarized the importance of luminescent oxygen sensing for biological detection, especially for determination of respiration rates. So far, such rates were determined predominantly in static cell cultures. Systems for their measurement have been commercialized and are considered as benchmarks [25,26]. Agilent's MitoXpress platform utilizes standard 96-well plates, sealed with mineral oil, in which oxygen and pH probes are dispersed to determine acidification and respiration rates. The assay volume (150 µL) of this system leads to assay times between 30–60 min and the potential extraction of lipophilic substances into the mineral oil layer is problematic. Agilent's XF analyzer platform uses a special microplate, where a cartridge is pressed down to seal off a small chamber (7 µL) at the bottom of the well. Additionally, the system has four injector ports to deliver reagents to the well. Nevertheless, it cannot constantly deliver fresh cell media and it is not possible to simulate concertation profiles and gradients. Both described systems apply static cell culturing conditions, which mimic physiological conditions only to a certain extent and lack resemblance in terms of shear stress or biomarker concentration. This leads to a demand in sensor technology capable to perform such experiments in microfluidic cell cultures and organ-on-chip applications.

Nowadays, the majority of such systems utilize PDMS as substrate for microfluidic chips. The problem with this material is, next to its known absorbance properties for biomarkers and drugs due to its lipophilic nature [27,28], its high oxygen permeability which does not allow viable oxygen or respiration measurements. For this purpose, thermoplastic polymer materials with low oxygen permeability, like polyethylene terephthalate (PET), polycarbonate (PC), cyclic olefin copolymer (COC), or even polystyrene (PS), are required as chip material. Prototyping of thermoplastic materials is however quite challenging and are usually fabricated with industrial techniques such as injection molding.

Herein, we present a microfluidic chip made from thermoplastic COC with low gas permeability via an innovative prototyping strategy, equipped with luminescent oxygen and pH sensor spots. With these sensor spots, it is not only possible to monitor the pH and the oxygen concentration inside the microfluidic cell chamber, but via stop/flow measurements, also determine the respiratory and acidification rates of mammalian cells.

2. Material and methods

2.1. Sensor material

The aza-BODIPY pH indicator dye 4-(5,5-difluoro-7-(4-hydroxyphenyl)-1,9-diphenyl-5*H*-5λ^4,6λ^4-dipyrrolo[1,2-*c*:2′,1′-*f*][1,3,5,2]triazaborinin-3-yl)-*N*-dodecylbenzamide (compound 5; OHC12) [29] and microcrystalline powder of silanized Egyptian Blue [30], were synthesized in our lab as previously described. Poly-*tert*-butylstyrene particles (ptBS particles) stained with 2 % (w/w) oxygen sensitive platinum (II)-*meso*-tetra(4-fluorophenyl)tetrabenzoporphyrin (PtTPTBPF) were prepared as described elsewhere [31]. Hydromed D4, a polyurethane based hydrogel, purchased from AvanSource biomaterials was used as matrix polymer. Buffer substances were bought from Carl Roth GmbH and used without further purification.

2.2. Microfluidic chip

2.2.1. Microfabrication

A master of the microfluidic chip was 3D printed, consisting of four channels with two cell chambers each. With a channel height of 280 µm and a surface area of 18 mm^2 for each chamber, this leads to a chamber volume of 5 µL (for further details of the chip dimensions see supporting info Figure SI1). Via electroplating and resulting Ni deposition, a negative master copy was produced. This negative master has the dimensions of standardized optical media (CD's, DVD's) and was inserted in regular injection molding machines used for their production. COC was used for the performed experiments due to its low oxygen permeability, high transparency and low auto-fluorescence over a wide spectral range [32]. Post-processing of the obtained green bodies is necessary, since with this fast prototyping technique no structures deeper than 250 µm can be produced.

The post-processing step includes the manual cutting of the top part (= structured part) of the microfluidic chips from the discs and drilling of holes (Ø2 mm) for positioning. Further, the surface of the microfluidic chip was scratched with a drill and the chip holder used as a stencil to mark the exact positions of the sensor spots and increase their adhesion. This led to a pattern of two spots per chamber, which was later matched by the arrangement of the optical fibers via the optic block of the chip holder. After sensor integration (described in 2.3) holes with a diameter of 2.5 mm were drilled and pieces of Tygon R3607 tubing (2.33 mm OD, 0.51 mm ID; Ismatec, IDEX Corporation, Switzerland) were glued into the holes in order to provide ports for the microfluidic system.

2.2.2. Chip bonding

Chips were bonded using 80 µm thick double-sided adhesive tape ARcare 90445 (Adhesive Research). The microfluidic channels were cut out using a CAMM-1 Gs24 cutting plotter (Roland, Germany) equipped with carbide blades (ZEC-U3017; Roland, Germany). The structured tape was removed from the substrate liner, aligned with the structured part of the microfluidic chip (upper half) and manually laminated to ensure proper bonding. After removal of the remaining protective lining layer, the chips were sterilized with the UV lamp of a lamina flow workbench and sealed with a 240 µm thick Topas COC foil (Denz Biomedical GmbH, Austria) under aseptic conditions.

2.3. Sensor integration

A microdispenser MDS3200+ from VERMES Microdispensing GmbH, equipped with a 70 µm nozzle and a tungsten tappet with a tip diameter of 0.7 mm, was used for sensor integration. It was mounted on a custom-made CNC platform, which was controlled via Linux CNC and allowed exact positioning of the sensor spots. The used printing parameters for oxygen and pH sensors spots are shown in table SI1 in the supporting information.

The pH sensor formulation consists of 0.33 mg of OHC12 dye and 54.8 mg of Egyptian Blue which were suspended in 1380 mg of a solution of hydrogel Hydromed D4 (8 % w/w) in THF/water (9 + 1). Homogenization was done with a Sonifier from Branson with ten pulses (1 s) with nine second cooldown intervals. After evaporation of the solvents the resulting sensor spot consisted of 0.2 % w/w indicator dye (OHC12), 33.3 % w/w reference dye (Egyptian Blue) and 66.5 % w/w host polymer (hydrogel Hydromed D4).

For the O_2 sensor formulation 82.5 mg ptBS particles, stained with 2 % PtTPTBPF, were suspended in 1650 mg of a hydrogel Hydromed D4 solution (5 % w/w) in isopropanol/water (3 + 1). The mixture was homogenized with a Sonifier from Branson and the resulting sensor consisted of 50 % w/w ptBS particles and 50 % w/w hydrogel Hydromed D4 after evaporation of the solvents leading to a relative Pt-dye concentration of 1 % w/w.

2.4. Sensor stability

Sensor stability was tested for the pH sensor spots by submerging an unclosed microfluidic chip with the chip holder into a beaker containing a buffer solution made from 10 mM Tris, 10 mM BisTris, 150 mM NaCl and 1.5 mM NaN_3 (preventing microbiological growth). The buffer was kept at 37 °C and alkaline solution (300 mM NaOH with 10 mM Tris and 10 mM BisTris) and acidic solution (300 mM HCl with 10 mM Tris and 10 mM BisTris) were added automatically with a Cavro Centris pump from Tecan to adjust the pH. The pH was measured with a glass pH electrode and a NaCl filled reference electrode from Idronaut. The stability test ran for 10 days at pH 7.5 and once a day a calibration between pH 5 and 9 was done with 18 distinct pH values. The read-out of the sensor spots was conducted with a miniaturized phasefluorimeter (Firesting) from Pyroscience equipped with 1-meter-long, polished POF 1/2.2 mm fibers. The measurement settings can be found in table SI2 (supporting info). The cotangents of the measured phase angles were plotted against the pH values and the calibration function was obtained by fitting with a Boltzmann equation (Eq. 1) where *A* represents the top value under acidic conditions, *B* the bottom value under basic conditions, pK_a the apparent pK_a value and *slope* the slope at the pK_a value.

$$\cot(d\varphi) = B + \frac{A - B}{1 + 10^{\frac{pH - pKa}{slope}}} \quad (1)$$

For the oxygen sensor spots no distinct durability tests were performed since their stability has been shown in previous reports [17,19,23].

2.5. Set up

A chip holder was constructed in order to guarantee a good alignment of the optical fibers from the read-out device with the sensor spots in the microfluidic channels. The holder consists of a frame holding the chip and an optic block which positions the fibers. The optic block can be removed in order to allow visual inspection of the cells in the fluidic chamber via microscope. A CAD drawing of the holder can be found in the supporting information (Figure SI2). Since eight chambers, with two spots each, were incubated in parallel on one chip, read-out was done with four separate four-channel Firesting phasefluorimeters from Pyroscience equipped with 1 m polished POF 1/2.2 mm fibers. The optical fibers were used to guide the sinusoidal modulated 620 nm excitation light to the sensor spot and collect the delayed emission light (NIR) simultaneously. The chip holder with the microfluidic chip was placed on a heated stage with integrated temperature control, which was set to 37 °C. For fluid transport, a four-syringe KDS 250 syringe pump (KD Scientific, USA) was used with 20 mL glass syringes (ILS, Germany) connected to 1/32" PEEK tubing (ID = 0.015", Ismatec, Germany) via 4-way PEEK valves (IDEX Health & Science, USA). A microfluidic bubble trap system, comprising of nine circular 1 mm diameter trapping wells (250 µm height), was connected via 50 cm long 1/32" PEEK tubing used as preheating, as well as bubble trapping unit. The bubble trap was then further connected with the cultivating chambers via 4 cm long 1/32" PEEK tubing. This led to a total dead volume before the cell chamber of around 65 µL. A picture of the assembled set-up is shown in Figure SI3 (supporting information).

2.6. Calibration

2.6.1. O_2

Since the used sensor material was the same used by Nacht et al. [31], their calibration data were used as factory setting for the oxygen sensor spots. A two-point calibration at anoxic conditions and air-saturated conditions was performed for one spot at 37 °C in cell medium to account for the slight changes environment and used for all oxygen sensor spots. Anoxic conditions were established by adding $NaSO_3$, air saturated conditions by shaking the medium right before measurement. The measurement settings for the phase fluorimeter can be found in table SI2 (supporting information).

2.6.2. pH

Calibration of the pH sensor spots was performed with 10 % FCS supplemented cell culture medium (Gibco) spiked with 10 mM of a buffer substance (acetate, MES, TRIS or glycin) between pH 4.5 and pH 10. The buffer substance with the appropriate pK_a value was dissolved in the media, the pH adjusted with 1 M NaOH or 1 M HCl at 37 °C and afterwards filtered through a 0.45 µm sterile filter (VWR, Austria). A list with the used buffers and their pH can be found in table SI3 in the supporting information. The buffers were transferred under aseptic conditions within a laminar-flow cabinet into 20 mL glass syringes and manually flushed through the microfluidic chip. The measurement settings for the phasefluorimeter can be found table SI2 (supporting information).

2.7. Cell seeding

2.7.1. Pretreatment

In order to get aseptic surfaces in the microfluidic chips, the structured parts, containing the sensor spots, were treated with UV light (λ~250 nm) from the laminar flow workbench for 15 min prior to chip bonding. Microfluidic tubing, valves, the double adhesive tape and the COC foil were disinfected with 70 % ethanol. In a second step, the COC foil was treated with ambient oxygen plasma for 10 min using a plasma chamber (Harrick Plasma, USA) equipped with an Equinox pressure control unit (Blackhole Lab, France) for 2 min at 450 mTorr to enhance cell adhesion on the polymer surfaces. The chip was bonded according to Section 2.2.2. at aseptic conditions. To promote cell adhesion, the cell culture chambers were treated with a 1% collagen I (Sigma Aldrich) solution in PBS (Sigma Aldrich) for one hour. In the next step, the chips were flushed with supplemented RPMI 1640 medium (Gibco) and the sensor spots were calibrated as described in Section 2.6.

2.7.2. Seeding and incubation

A549 human lung carcinoma epithelial-like cell line (ATCC Nr.: CCL-185) were cultured in a RPMI 1640 Medium (Gibco) supplemented with 10 % fetal bovine serum, L-glutamine, and 1 % antibiotic/antimycotic solution. The trypsinized cells, with a concentration of 10^6 cells/mL,

were seeded into the calibrated microfluidic chips and adhesion was observed under the microscope. The oxygen concentrations within the chambers were monitored via the sensor spots, to prevent oxygen limitation. After 4 h, cell seeding was complete and a confluent cell layer was formed. The cells were cultivated within the chip at a temperature of 37 °C and with constant perfusion of media of 10 µL/min, which represents a flow velocity of 11.9 µL/min*mm^2. Cell density was evaluated by counting cells stained with Hoechst 33342 fluorescent dye with ImageJ software after the end of the experiments.

2.8. Acidification and respiration rate measurement

The acidification and respiration rate of the cells were analyzed by stopping the flow for approximately 30 min. Afterwards the flow was turned on again (10 µL/min) and the chip flushed with fresh media until the oxygen saturation and pH level returned to normal.

In order to detect a change in the metabolism, the cells were treated with FCCP (Carbonyl cyanide-4-(trifluoromethoxy)phenylhydrazone from Sigma Aldrich) which leads to an upregulation of the respiratory rate and the acidification rate [24]. The cells were incubated with media spiked with 0.5, 5 and 20 µM FCCP for 5.5 h and the acidification rates and respiration rates measured multiple times. At end of the experiment the cell density was evaluated, as previously described, and the consumption rates corrected for the determined cell count.

3. Results & discussion

3.1. Sensor materials

The sensor materials are chosen according to previous experiences and reports and are immobilized in a hydrogel matrix (Hydromed D4). This swell able material is FDA approved and designed in a way so proteins do not adhere to it. Therefore, it is not possible for cells to grow on it, effectively shielding the sensitive dyes from the cells and eliminating otherwise possible interactions. No adverse effects of the sensor material to the cells thus has been observed so far (Figure SI6, supporting information).

Oxygen measurements are performed with polymer particles stained with PtTPTBPF since they have proven their stability and suitability for measurements in biological systems multiple times [17,23,31]. They can be excited with red light (620 nm) and emit in the near infrared (NIR) part of the electromagnetic spectrum. The lifetime of the excited dye molecule is proportional to the oxygen partial pressure and is used as a robust, intensity independent parameter.

The pH sensitive OHC12 dye has a reported apparent pK_a value of 7.59 in hydrogel Hydromed D4 [29] and is therefore perfectly suited to monitor the decrease in pH in cell culture media from pH 7.5 to pH 6.5. It is used together with inert and phosphorescent Egyptian Blue particles, which serve as reference material due to similar spectral properties, to enable dual-lifetime referenced (DLR) measurements [33,34]. This technique is reportedly more robust than simple intensity measurements and therefore small changes in pH can be detected more reliably. The pH indicator and the reference material both can be excited with red light (620 nm) and emit light in the NIR part of the electromagnetic spectrum. The stability of the pH sensor spots at 37 °C was investigated over 10 days. The daily calibration points are fitted with a Boltzmann equation (Eq.1) and the respective curves are shown in Fig. 1. The resolution of the pH sensor spots has been calculated to be 0.003 pH units with a response time t_{95} of around 30 s for a pH shift of 0.5 pH units from pH 7 to pH 7.5. A slight drift of about 0.01 pH units per day can thereby be observed at the point of inflection. This drift is acceptable, keeping in mind that only the relative change of the pH over two minutes is measured to determine the acidification rate.

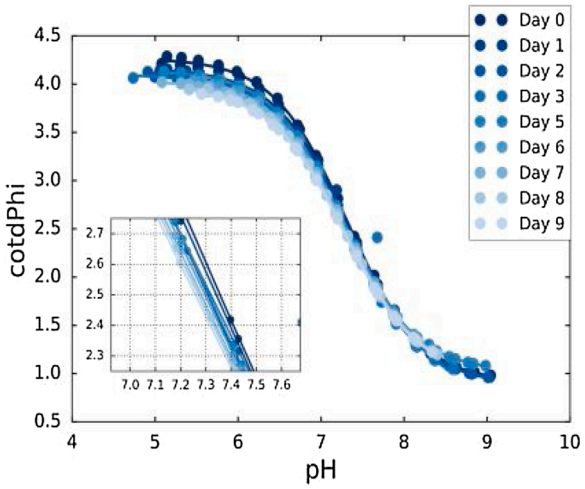

Fig. 1. Sigmoidal calibration curves of a pH sensor spot in the course of 10 days. A shift in the apparent pK_a of around 0.01 pH unit per day can be observed.

3.2. Microfluidic chip fabrication and sensor integration

PDMS is the most common material for microfluidic chips for cell conditioning. The material is known for its ease of fabrication and its excellent oxygen permeability, leading to air-saturated conditions in the cell media. However, PDMS is also known for its unspecific binding of substances due to the lipophilic character of the material [27,28]. In order to be able to perform respiration measurements, an oxygen impermeable chip material was used. COC has an oxygen permeability of 18.52 cm^3*mm/m^2 day atm [35], very good optical properties and good biocompatibility and is consequently a suitable material for respiration measurements of cells in a microfluidic device. Therefore, the injection molded structured part of the chip, as well as the cover foil is fabricated from this material. However, processing of thermoplastic materials is significantly more effort when, due to small chip numbers, fabrication methods for mass production are not an option. This problem is addressed by utilizing a novel fast prototyping method.

The method allows the fabrication of microfluidic green bodies made from thermoplastic materials, utilizing conventional injection molding machines for optical media such as compact discs. Manufacturing of the needed inlays comes at reasonable costs even for small series of prototype chips. Therefore, a master chip gets covered with nickel via electroplating, forming the inlay yielding a negative master of the chip structure. The technique is compromised by a limited structural height of 250 µm and therefore no possibility for holes. Fig. 2b shows the 200 µm deep structure of the designed chip, whereas in Fig. 2c a ready-made green body can be seen. Subsequently, the chips have to be cut out from the disc and holes for positioning and the fluidic ports have to be drilled during post-processing. Further the substrate was scratched with a drill and the chip holder used as a stencil at the exact locations where the sensor spots are afterwards placed. This marks enable the exact positioning of the spots and subsequently allow the alignment with the optical fibers. Moreover, the rough mark improves the adhesion of the hydrogel-based sensor spot to the smooth COC surface by enhancing the mechanical link between the two materials.

The sensor material is deployed into the chambers of the chip via so called microdispensing. This technique utilizes a piezoelectrically driven tappet to mechanically force the sensor formulation through a nozzle. With this method, viscos solutions and dispersions can be processed. This is key for processing the pH sensor formulation, since it needs to be quite viscous to prevent fast sedimentation of the ceramic reference particles. It allows using particle sizes up to 10 µm in diameter and is capable of printing into chambers and channels of microfluidic

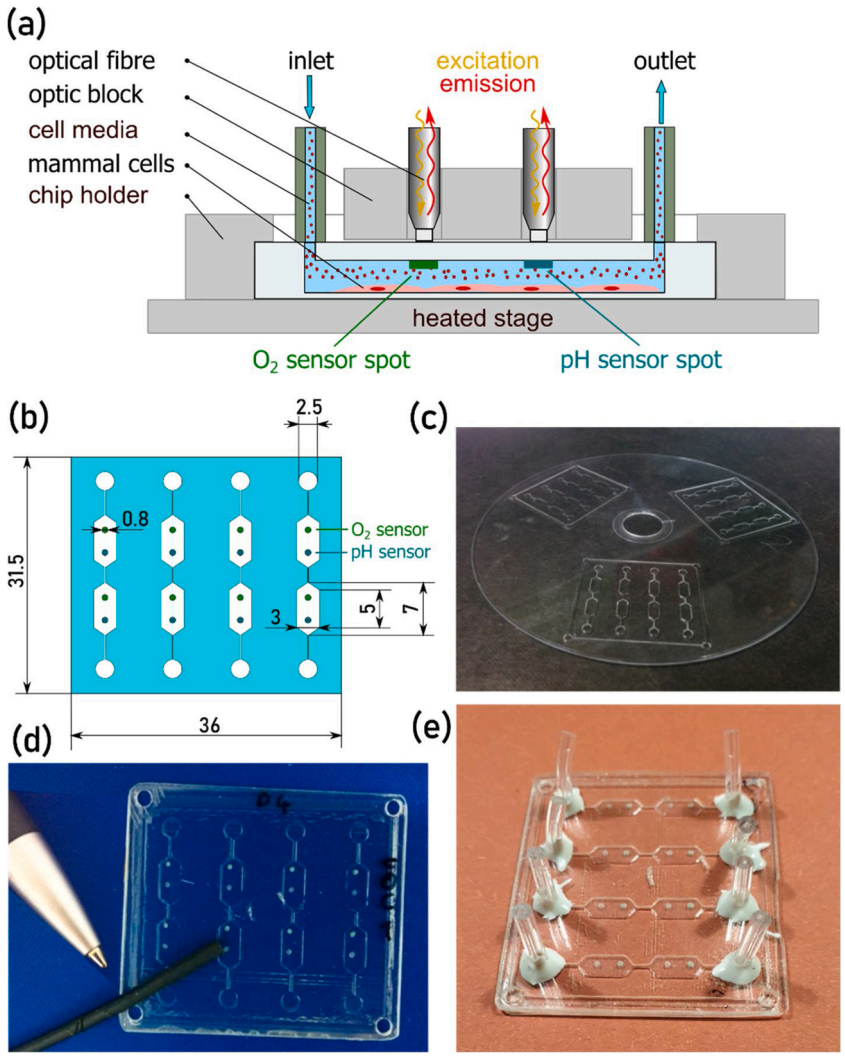

Fig. 2. Different development stages of the microfluidic chip; (a) Utilized concept of the microfluidic chip; (b) Sketch of the prototype after which the 3D print is modeled; (c) Green body of the chip in shape of an optical media after injection molding; (d) Structured part of the chip after drilling of positioning holes and sensor integration; (e) Fully assembled microfluidic chip with ports before collagen treatment.

devices, which cavities can be as deep as 5 mm. Depending on the settings and sensor formulation, sensor spots as small as 500 µm can be printed. The dispenser is mounted on a custom-made CNC platform allowing exact positioning of the sensor spot. Since the optical fibers used for read-out have an inner diameter of 1 mm, the goal is to produce spots, which are smaller, so the entire spot contributes to the signal and inhomogeneities within one spot do not affect it. Therefor the print parameters were optimized in a way to produce spots with an average size of 0.8 mm and an approximate height of 4 µm (in the dry state) fulfilling this requirement. Fig. 2d shows the chip after sensor integration and allows for a size comparison between the optical fiber and the sensor spot.

The simple port system is fabricated utilizing pieces of Tygon tubing. They are glued into holes drilled in the structured part of the chip. The inner diameter (0.51 mm) of this flexible material is a little bit smaller than the outer diameter (0.79 mm) of the PEEK tubing, used for connecting the fluidic system, allowing a tight fit. The chips are closed using a double-sided adhesive tape from which the structure of the microfluidic channels has been previously removed. It is 80 µm thick and contributes to the total height of the microfluidic structure. After laminating the tape onto the structured part of the chip it is disinfected with UV light. The COC cover foil is treated with ambient oxygen plasma to disinfect it and activate its surface at the same time. The chip is afterwards assembled in a laminar flow workbench, treated with collagen and the ports are closed with disinfected plugs. The chips are stored this way until they are calibrated right before use. An assembled chip right before the collagen treatment is shown in Fig. 2e. The homogeneity of the flow conditions inside the microfluidic cell chamber has been calculated with Autodesk CFD 2019 and is displayed in the supporting information (Figure SI8).

3.3. Set-up characterization

In order to gain stable signals, a good alignment between the optical fiber and the sensor spot must be guaranteed. Therefore, a chip holder was manufactured, consisting of a frame for positioning the microfluidic chip and an optical block, which supports the polished POF fibers. The frame features a pocket at the bottom in which the microfluidic chip is positioned with four pins. The pocket has the same height as the chip and therefore presses it down when assembled on a heated stage. The window in the frame is big enough to enable microscopic inspection of the cell chambers and allow connection of the tubing to the chip. The optic block is positioned with four bolts and screw nuts in the optical window. It holds up to 16 POF fibers (two for each cell chamber) and presses them onto the topside of the chip right above the sensor spots. The CAD drawing of the chip holder is shown in figure SI2 (supporting

information).

In order to minimize bubble formation during incubation, all culture media is degassed at 37 °C and stored in glass syringes. Further, a bubble trap is deployed right before the cell chamber in order to preheat the media and capture bubbles before entering the microfluidic chamber during incubation.

The pH sensor spots are calibrated by fitting the measurement points with the Boltzmann equation (Eq.1). Fig. 3 shows the calibration curves for all eight pH sensor spots of one microfluidic chip. The maximal value under acidic conditions (top value A) is different for each spot due to small variations in the ratio between the indicator dye and the reference particles. These inhomogeneities of the sensor material are caused during the microdispensing process of the dispersion due to the density difference between the polymer solution and the ceramic reference particles. However, the fluctuation of the top value barely influences the apparent pK_a (values displayed in Fig. 3) leading to similar sensor characteristics. The pH measurements of the cell cultures are carried out between pH 7.5 and 6.8 and are therefore perfectly covered by the pH sensors linear range.

3.4. Cell cultivation

The microfluidic chip is treated with collagen after assembling to guarantee a fast cell adhesion. (<4 h). The oxygen levels during the seeding procedure are monitored with the oxygen sensor spots to ensure a sufficient O_2 supply. The oxygen concentration did not decrease under 22 hPa (≙ 10 % air saturation). During cell seeding, the calculated oxygen consumption per 10^3 cells was 0.024 ± 0.015 hPa/min compared to 0.85 ± 0.12 hPa/min after cell attachment (time = 0, Fig. 7a). During adhesion, the cells are in a state of low metabolic activity, which explains the low oxygen consumption rate before cells are attached to the surface [36]. Fig. 4a shows a microscopic image of A549 cells just before starting the incubation flow 3.5 h after seeding, confirming a dense layer of adhered cells combined with non-adhered excess cells.

A549 human lung carcinoma epithelial-like cell line is a robust model system with a high metabolic activity and is therefore a suitable model for toxicological screening [37].

3.5. Acidification and respiration rate measurements

The cells are incubated with a flow of 10 µL/min, guaranteeing air saturation of the cell media and therefore a sufficient oxygen supply for the cells. The incubation flow is interrupted for the acidification and respiration measurements and the decrease in oxygen and pH is monitored. Fig. 5 shows four consecutive measurements conducted 44 h after cell seeding. The flow of culture media is stopped for approximately 30 min, without letting the oxygen concentration decrease below 10 % air saturation (22 hPa). As confirmed by the microscopic images, the cell concentration in the second chamber (pO_2 Ch 2−2) is higher than in the first chamber (pO_2 Ch 2−1) leading to a faster decrease of pO_2, respectively a steeper slope. Interestingly, the oxygen saturation in the second chamber does not reach air saturation, even during the incubation flow. This is probably due the respiratory behavior of the cells in the first chamber and shows how oxygen impermeable the used system is. The effect of metabolic activity of the cells in the first chamber can also be observed through the slightly lower pH during incubation flow in the second chamber. However, this effect is way less pronounced for pH.

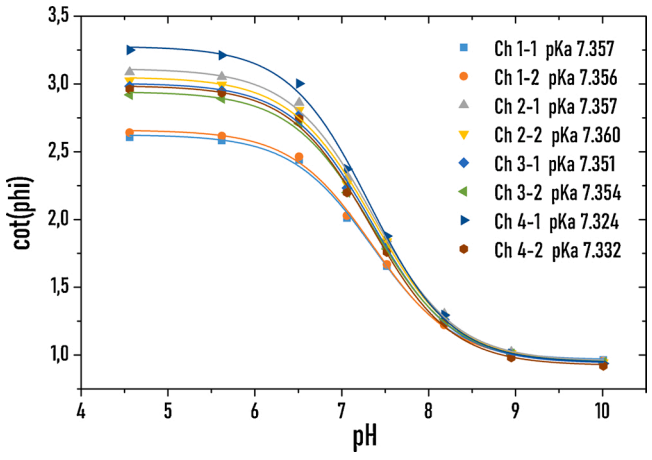

Fig. 3. Sigmoidal calibration curves of eight pH sensor spots located in one chip showing different top values but similar apparent pK_a values.

To calculate the acidification and respiration rates, the slopes of the decrease after stopping the incubation flow, are analyzed. The first 60 measurement points (e.g. two minutes) show the most stable results and are therefore optimal to determine the respiration and acidification rates (see figure SI4 and SI5, supporting information). Fig. 6 shows two sets of measurements from channel 2, conducted 18 and 44 h after seeding with multiple measurements conducted at each point. Evidently, the repeatability of the measurement is high and only minor differences are visible, showing the robustness of this method. Within each set, a measurement was done every 30 min. Since the cell concentration was different between the two chambers, the respiration and acidification rates are different as well. Interestingly, the gap between the difference in acidification rate and respiration rate is not equal. This is probably due to a varying buffer capacity of the media in the chamber originating from a different initial pH value.

To show the potential of the oxygen and pH sensor spots for the evaluation of the metabolism of viable cells, A549 cells are incubated with FCCP and their response is monitored. FCCP is a compound known for is upregulating effect on the respiration and acidification rate [24]. This effect can be reproduced in the conducted toxicity study shown in Fig. 7. After seeding and an initial growth phase, three chambers are incubated with different concentrations of FCCP. A strong increase in the acidification and respiration rate can be observed for the concentrations of 0.5 and 5 µM. However, for the chamber incubated with 20 µM the respiration rate decreased with time during perfusion while the acidification rate remained as before FCCP treatment. FCCP is known to disrupt ATP synthesis [38], which could be an explanation to the decrease in pH at concentrations of 0.5 and 1 µM. At 40 µM, FCCP causes complete disruption of cellular microtubules leading to a disruption of the ATP synthesis in mitochondria as well as the induction of apoptosis [39]. These changes in cell viability are reflected by the decreased oxygen consumption rate during perfusion with 20 µM.

4. Conclusion and outlook

In conclusion, we were able to introduce luminescent pH and oxygen sensors into microfluidic systems, which are sensitive enough to measure the acidification and respiration rate of cell cultures. Moreover, they showed excellent stability and can be used for at least 10 days without major drift. Further, the sensor material and the measurement had no effect on the cells and it can therefore be considered a non-invasive method. As shown in a previous work [18] the developed methodology can be used to monitor not only immortalized cell lines but also primary human cells such as human umbilical vein endothelial cells (HUVEC) and adipose-derived stem cells (ASC). By culturing cells under dynamic conditions, physiological stimulus similar to *in-vivo* conditions can be emulated and thus create more physiologically relevant models. Since this sensor technology can quite easily be implemented to other thermoplastic microfluidic systems and enables monitoring of cell metabolism, it can pave the way to a more standardized and controlled way of monitoring culture conditions within cell-based microfluidics and organs-on-a-chip systems. In this aspect, the usage of industrial manufacturing techniques for sensor integration is key, since it allows reproducible measurements for a large number of experiments. Microdispensing has shown its potential in this regard and can lead to the

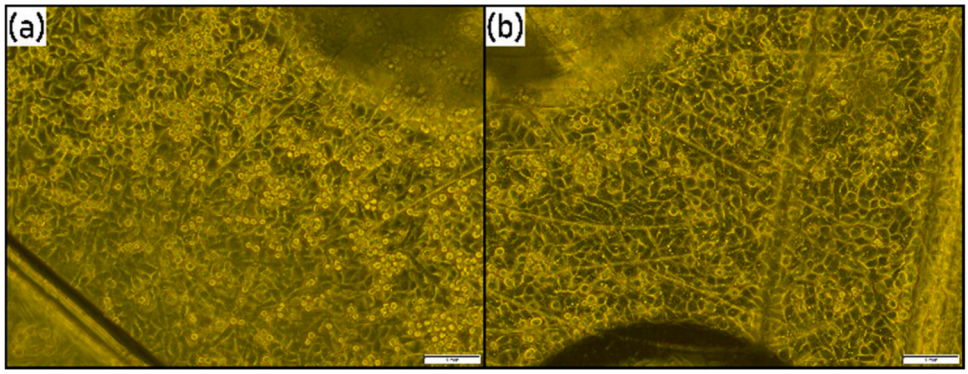

Fig. 4. Microscopic image of A549 cells in microfluidic cell chamber (a) before starting incubation flow 3.5 h after seeding and (b) after 12 h of incubation. The pH sensor spot, which is located at the topside of the chamber, is visible (out-of-focus) at the top of both images. Scale bar: 1 mm. 20x magnification.

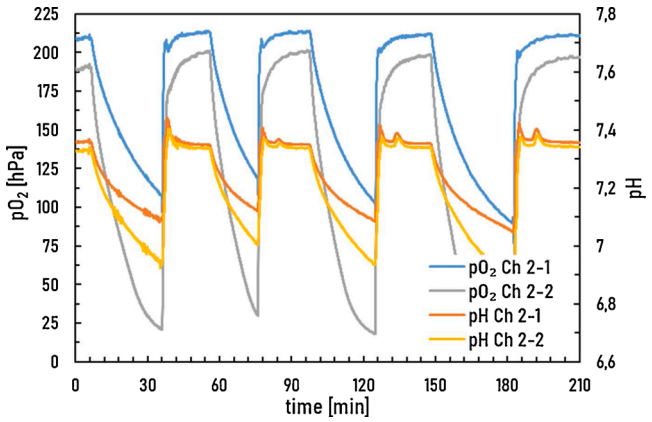

Fig. 5. Stop/flow measurements for the determination of acidification and respiration rates. Two consecutive chambers of one channel 44 h after seeding are shown.

integration of even more parameters in a single microfluidic unit. These complementary datasets are crucial for gaining deeper insights into cell metabolism and a better understanding of cell-drug interactions.

Further work will focus on the enhancement of the microfluidic system, improving channel dimensions, the port system, fabrication with more advanced techniques such as injection molding and improved bonding methods. Moreover, the optimization of the spotting process for pH sensors will enable a simpler calibration routine with 2-point or 1-point calibration. Overall, the goal is to improve the reliability and ease-of-use of the system to enable high-throughput data collection and subsequent comparison with existing data. On the long run, additional sensor spots for temperature, glucose and lactate should be developed and integrated in various microfluidic set-ups, enabling an even closer look into metabolic processes. This is of tremendous interest for 3D cell cultures and organ-on-chip systems, since there is a lack of inline analytical methods for the determination of the cell metabolism and monitoring of culture conditions.

CRediT authorship contribution statement

Bernhard Müller: Methodology, Investigation, Writing - original draft, Visualization. **Philipp Sulzer:** Methodology, Investigation. **Manuel Walch:** Methodology. **Helene Zirath:** Methodology, Investigation, Writing - review & editing, Supervision. **Tomáš Buryška:** Investigation, Writing - review & editing. **Mario Rothbauer:** Writing - review & editing, Supervision. **Peter Ertl:** Resources, Funding acquisition. **Torsten Mayr:** Conceptualization, Resources, Writing - review & editing, Supervision, Project administration, Funding acquisition.

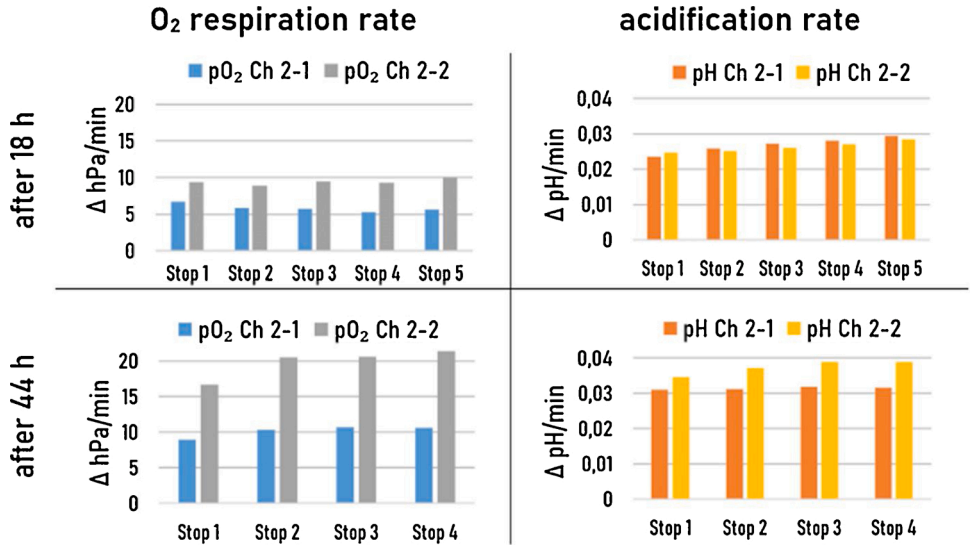

Fig. 6. Respiration and acidification rates of A549 human lung carcinoma epithelial-like cell line at 18 and 44 h after seeding. Repeated measurements are performed every 30 min.

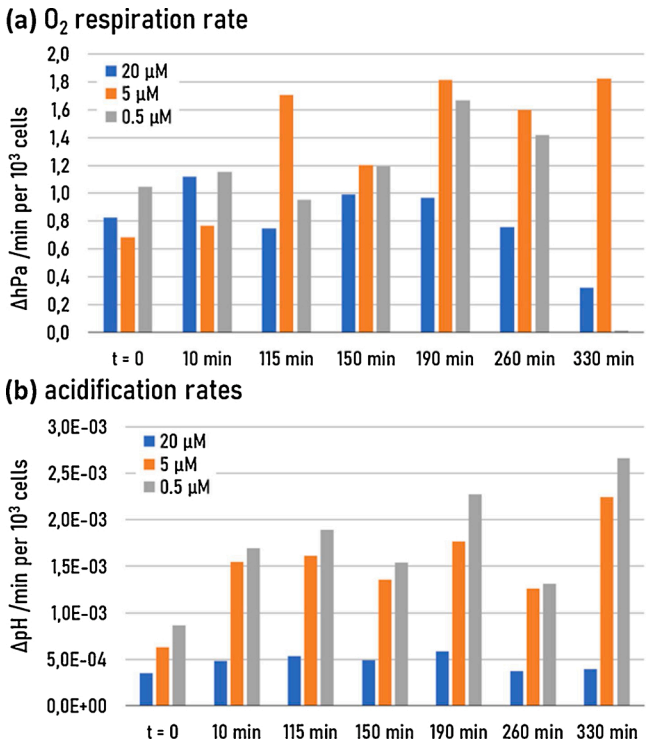

Fig. 7. Development of respiration (a) and acidification (b) rates of A549 human lung carcinoma epithelial-like cell line during incubation with three different concentrations of FCCP.

Declaration of Competing Interest

The authors declare that they have no known competing financial interests or personal relationships that could have appeared to influence the work reported in this paper.

Acknowledgments

Financial support by the Austrian Research Promotion Agency (FFG) in the project NextGenUpCon (Project number 849791) is gratefully acknowledged. TB would like to acknowledge the FEMS research grant (FEMS-RG-2016-0057).

Appendix A. Supplementary data

Supplementary material related to this article can be found, in the online version, at doi:https://doi.org/10.1016/j.snb.2021.129664.

References

[1] J.H. Sung, Y.I. Wang, N. Narasimhan Sriram, M. Jackson, C. Long, J.J. Hickman, M. L. Shuler, Recent advances in Body-on-a-chip systems, Anal. Chem. 91 (2019) 330–351, https://doi.org/10.1021/acs.analchem.8b05293.

[2] Y.S. Zhang, J. Aleman, S.R. Shin, T. Kilic, D. Kim, S.A. Mousavi Shaegh, S. Massa, R. Riahi, S. Chae, N. Hu, H. Avci, W. Zhang, A. Silvestri, A. Sanati Nezhad, A. Manbohi, F. De Ferrari, A. Polini, G. Calzone, N. Shaikh, P. Alerasool, E. Budina, J. Kang, N. Bhise, J. Ribas, A. Pourmand, A. Skardal, T. Shupe, C.E. Bishop, M. R. Dokmeci, A. Atala, A. Khademhosseini, Multisensor-integrated organs-on-chips platform for automated and continual in situ monitoring of organoid behaviors, Proc. Natl. Acad. Sci. U. S. A. 114 (2017) E2293–E2302, https://doi.org/10.1073/pnas.1612906114.

[3] C. Oleaga, A. Riu, S. Rothemund, A. Lavado, C.W. McAleer, C.J. Long, K. Persaud, N.S. Narasimhan, M. Tran, J. Roles, C.A. Carmona-Moran, T. Sasserath, D. H. Elbrecht, L. Kumanchik, L.R. Bridges, C. Martin, M.T. Schnepper, G. Ekman, M. Jackson, Y.I. Wang, R. Note, J. Langer, S. Teissier, J.J. Hickman, Investigation of the effect of hepatic metabolism on off-target cardiotoxicity in a multi-organ human-on-a-chip system, Biomaterials 182 (2018) 176–190, https://doi.org/10.1016/j.biomaterials.2018.07.062.

[4] C. Oleaga, C. Bernabini, A.S.T. Smith, B. Srinivasan, M. Jackson, W. McLamb, V. Platt, R. Bridges, Y. Cai, N. Santhanam, B. Berry, S. Najjar, N. Akanda, X. Guo, C. Martin, G. Ekman, M.B. Esch, J. Langer, G. Ouedraogo, J. Cotovio, L. Breton, M. L. Shuler, J.J. Hickman, Multi-Organ toxicity demonstration in a functional human in vitro system composed of four organs, Sci. Rep. 6 (2016), https://doi.org/10.1038/srep20030.

[5] F. Qian, C. Huang, Y.-D. Lin, A.N. Ivanovskaya, T.J. O'Hara, R.H. Booth, C.J. Creek, H.A. Enright, D.A. Soscia, A.M. Belle, R. Liao, F.C. Lightstone, K.S. Kulp, E. K. Wheeler, Simultaneous electrical recording of cardiac electrophysiology and contraction on chip, Lab Chip 17 (2017) 1732–1739, https://doi.org/10.1039/C7LC00210F.

[6] B.M. Maoz, A. Herland, O.Y.F. Henry, W.D. Leineweber, M. Yadid, J. Doyle, R. Mannix, V.J. Kujala, E.A. FitzGerald, K.K. Parker, D.E. Ingber, Organs-on-Chips with combined multi-electrode array and transepithelial electrical resistance measurement capabilities, Lab Chip 17 (2017) 2294–2302, https://doi.org/10.1039/C7LC00412E.

[7] M. Stancescu, P. Molnar, C.W. McAleer, W. McLamb, C.J. Long, C. Oleaga, J.-M. Prot, J.J. Hickman, A phenotypic in vitro model for the main determinants of human whole heart function, Biomaterials 60 (2015) 20–30, https://doi.org/10.1016/j.biomaterials.2015.04.035.

[8] E. Moutaux, B. Charlot, A. Genoux, F. Saudou, M. Cazorla, An integrated microfluidic/microelectrode array for the study of activity-dependent intracellular dynamics in neuronal networks, Lab Chip 18 (2018) 3425–3435, https://doi.org/10.1039/C8LC00694F.

[9] D. Elbrecht, C. Long, J. Hickman, Transepithelial/endothelial Electrical Resistance (TEER) theory and applications for microfluidic body-on-a-chip devices, J. Rare Dis. Res. Treat. 1 (2016) 46–52, https://doi.org/10.29245/2572-9411/2016/3.1026.

[10] Y.I. Wang, H.E. Abaci, M.L. Shuler, Microfluidic blood–brain barrier model provides in vivo-like barrier properties for drug permeability screening, Biotechnol. Bioeng. 114 (2017) 184–194, https://doi.org/10.1002/bit.26045.

[11] M.B. Esch, H. Ueno, D.R. Applegate, M.L. Shuler, Modular, pumpless body-on-a-chip platform for the co-culture of GI tract epithelium and 3D primary liver tissue, Lab Chip 16 (2016) 2719–2729, https://doi.org/10.1039/C6LC00461J.

[12] F.A. Alexander, S. Eggert, J. Wiest, Skin-on-a-Chip: transepithelial electrical resistance and extracellular acidification measurements through an automated air-liquid interface, Genes 9 (2018) 114, https://doi.org/10.3390/genes9020114.

[13] A. Moya, M. Ortega-Ribera, X. Guimerà, E. Sowade, M. Zea, X. Illa, E. Ramon, R. Villa, J. Gracia-Sancho, G. Gabriel, Online oxygen monitoring using integrated inkjet-printed sensors in a liver-on-a-chip system, Lab Chip 18 (2018) 2023–2035, https://doi.org/10.1039/C8LC00456K.

[14] I.A. Ges, B.L. Ivanov, D.K. Schaffer, E.A. Lima, A.A. Werdich, F.J. Baudenbacher, Thin-film IrOx pH microelectrode for microfluidic-based microsystems, Biosens. Bioelectron. 21 (2005) 248–256, https://doi.org/10.1016/j.bios.2004.09.021.

[15] R. Riahi, S.A.M. Shaegh, M. Ghaderi, Y.S. Zhang, S.R. Shin, J. Aleman, S. Massa, D. Kim, M.R. Dokmeci, A. Khademhosseini, Automated microfluidic platform of bead-based electrochemical immunosensor integrated with bioreactor for continual monitoring of cell secreted biomarkers, Sci. Rep. 6 (2016) 1–14, https://doi.org/10.1038/srep24598.

[16] S.R. Shin, Y.S. Zhang, D.-J. Kim, A. Manbohi, H. Avci, A. Silvestri, J. Aleman, N. Hu, T. Kilic, W. Keung, M. Righi, P. Assawes, H.A. Alhadrami, R.A. Li, M. R. Dokmeci, A. Khademhosseini, Aptamer-based microfluidic electrochemical biosensor for monitoring cell-secreted trace cardiac biomarkers, Anal. Chem. 88 (2016) 10019–10027, https://doi.org/10.1021/acs.analchem.6b02028.

[17] S.L. Maldonado, P. Panjan, S. Sun, D. Rasch, A.M. Sesay, T. Mayr, R. Krull, A fully online sensor-equipped, disposable multiphase microbioreactor as a screening platform for biotechnological applications, Biotechnol. Bioeng. 116 (2019) 65–75, https://doi.org/10.1002/bit.26831.

[18] H. Zirath, M. Rothbauer, S. Spitz, B. Bachmann, C. Jordan, B. Müller, J. Ehgartner, E. Priglinger, S. Mühleder, H. Redl, W. Holnthoner, M. Harasek, T. Mayr, P. Ertl, Every breath you take: non-invasive real-time oxygen biosensing in two- and three-dimensional microfluidic cell models, Front. Physiol. 9 (2018), https://doi.org/10.3389/fphys.2018.00815.

[19] J. Ehgartner, P. Sulzer, T. Burger, A. Kasjanow, D. Bouwes, U. Krühne, I. Klimant, T. Mayr, Online analysis of oxygen inside silicon-glass microreactors with integrated optical sensors, Sens. Actuators B Chem. 228 (2016) 748–757, https://doi.org/10.1016/j.snb.2016.01.050.

[20] P. Gruber, M.P.C. Marques, N. Szita, T. Mayr, Integration and application of optical chemical sensors in microbioreactors, Lab Chip 17 (2017) 2693–2712, https://doi.org/10.1039/C7LC00538E.

[21] S.A. Pfeiffer, S. Nagl, Microfluidic platforms employing integrated fluorescent or luminescent chemical sensors: a review of methods, scope and applications, Methods Appl. Fluoresc. 3 (2015) 034003, https://doi.org/10.1088/2050-6120/3/3/034003.

[22] S. Sun, B. Ungerböck, T. Mayr, Imaging of oxygen in microreactors and microfluidic systems, Methods Appl. Fluoresc. 3 (2015) 034002, https://doi.org/10.1088/2050-6120/3/3/034002.

[23] I.B. Tahirbegi, J. Ehgartner, P. Sulzer, S. Zieger, A. Kasjanow, M. Paradiso, M. Strobl, D. Bouwes, T. Mayr, Fast pesticide detection inside microfluidic device with integrated optical pH, oxygen sensors and algal fluorescence, Biosens. Bioelectron. 88 (2017) 188–195, https://doi.org/10.1016/j.bios.2016.08.014.

[24] D.B. Papkovsky, R.I. Dmitriev, Biological detection by optical oxygen sensing, Chem. Soc. Rev. 42 (2013) 8700–8732, https://doi.org/10.1039/C3CS60131E.

[25] J. Hynes, T.C. O'Riordan, A.V. Zhdanov, G. Uray, Y. Will, D.B. Papkovsky, In vitro analysis of cell metabolism using a long-decay pH-sensitive lanthanide probe and

extracellular acidification assay, Anal. Biochem. 390 (2009) 21–28, https://doi.org/10.1016/j.ab.2009.04.016.
[26] D.A. Ferrick, A. Neilson, C. Beeson, Advances in measuring cellular bioenergetics using extracellular flux, Drug Discov. Today 13 (2008) 268–274, https://doi.org/10.1016/j.drudis.2007.12.008.
[27] M.W. Toepke, D.J. Beebe, PDMS absorption of small molecules and consequences in microfluidic applications, Lab Chip 6 (2006) 1484–1486, https://doi.org/10.1039/B612140C.
[28] R. Gomez-Sjoberg, A.A. Leyrat, B.T. Houseman, K. Shokat, S.R. Quake, Biocompatibility and reduced drug absorption of sol−Gel-Treated poly(dimethyl siloxane) for microfluidic cell culture applications, Anal. Chem. 82 (2010) 8954–8960, https://doi.org/10.1021/ac101870s.
[29] M. Strobl, T. Rappitsch, S.M. Borisov, T. Mayr, I. Klimant, NIR-emitting aza-BODIPY dyes – new building blocks for broad-range optical pH sensors, Analyst 140 (2015) 7150–7153, https://doi.org/10.1039/C5AN01389E.
[30] S.M. Borisov, C. Würth, U. Resch-Genger, I. Klimant, New life of ancient pigments: application in high-performance optical sensing materials, Anal. Chem. 85 (2013) 9371–9377, https://doi.org/10.1021/ac402275g.
[31] B. Nacht, C. Larndorfer, S. Sax, S.M. Borisov, M. Hajnsek, F. Sinner, E.J.W. List-Kratochvil, I. Klimant, Integrated catheter system for continuous glucose measurement and simultaneous insulin infusion, Biosens. Bioelectron. 64 (2015) 102–110, https://doi.org/10.1016/j.bios.2014.08.012.
[32] A. Piruska, I. Nikcevic, S.H. Lee, C. Ahn, W.R. Heineman, P.A. Limbach, C. J. Seliskar, The autofluorescence of plastic materials and chips measured under laser irradiation, Lab Chip 5 (2005) 1348, https://doi.org/10.1039/b508288a.
[33] C. Huber, I. Klimant, C. Krause, T. Werner, T. Mayr, O.S. Wolfbeis, Optical sensor for seawater salinity, Fresenius J. Anal. Chem. 368 (2000) 196–202, https://doi.org/10.1007/s002160000493.
[34] C. Huber, I. Klimant, C. Krause, O.S. Wolfbeis, Dual lifetime referencing as applied to a chloride optical sensor, Anal. Chem. 73 (2001) 2097–2103, https://doi.org/10.1021/ac9914364.
[35] T.E. Pedersen, Evaluation of Polymer Properties Influencing Oxygen Transfer Rates (OTR) in Microfluidic Cell Culture, Graz University of Technology. Master's Thesis, 2017.
[36] M. Rehberg, J.B. Ritter, Y. Genzel, D. Flockerzi, U. Reichl, The relation between growth phases, cell volume changes and metabolism of adherent cells during cultivation, J. Biotechnol. 164 (2013) 489–499, https://doi.org/10.1016/j.jbiotec.2013.01.018.
[37] U.G. Sauer, S. Vogel, A. Hess, S.N. Kolle, L. Ma-Hock, B. Van Ravenzwaay, R. Landsiedel, in vivo–in vitro comparison of acute respiratory tract toxicity using human 3D airway epithelial models and human A549 and murine 3T3 monolayer cell systems, Toxicology In Vitro 27 (2013) 174–190, https://doi.org/10.1016/j.tiv.2012.10.007.
[38] R. Benz, S. McLaughlin, The molecular mechanism of action of the proton ionophore FCCP (carbonylcyanide p-trifluoromethoxyphenylhydrazone), Biophys. J. 41 (1983) 381–398, https://doi.org/10.1016/S0006-3495(83)84449-X.
[39] B. Maro, M.C. Marty, M. Bornens, In vivo and in vitro effects of the mitochondrial uncoupler FCCP on microtubules, EMBO J. 1 (1982) 1347–1352.

Bernhard Müller is a post-doctoral researcher at the Institute of Analytical Chemistry and Food Chemistry at Graz University of Technology. He received his PhD in technical chemistry from Graz University of Technology (Austria). His research focuses on the development and integration of luminescent sensors into microfluidic systems as well as the utilization of luminescent sensors as a tool for concrete diagnostics.

Mario Rothbauer is a trained tissue engineer and obtained his doctorate biotechnology in 2015 at the University of Natural Resources and Life Sciences in Vienna BOKU (Austria) dealing with the development of lab-on-a-chip systems for cell-based biomedical applications. During his post doc at the Faculty of Technical Chemistry at the Vienna University of Technology he applied lab and organ-on-a-chip technology for the establishment of in-vitro organ models for drug and toxicological research. Currently, at the Department of Orthopaedics and Trauma Surgery of the Medical University of Vienna (Austria) he develops joint-on-a-chip systems for human musculoskeletal diseases including osteoarthritis.

Manuel Walch. After his PhD graduation in chemistry in 2016 at the University of Ulm, Germany, Manuel Walch started his career as project manager R&D at the kdg opticomp GmbH. In this position, he is active in several federally funded projects in the fields of μ-fluidics for lab-on-chip devices and micro-/nanostructures for optical applications.

Helene Zirath hold a MSc in Biotechnology from Lund University, Faculty of Engineering, and received her PhD in Technical Chemistry in 2016 at the Vienna University of Technology in Austria. She conducted her doctoral thesis at the Austrian Institute of Technology (AIT, Vienna) on the subject of lab-on-a-chip technology with a focus on point-of-care diagnostics for the detection of molecular biomarkers. Dr Zirath currently holds a postdoc position at the Cell-Chip group at Vienna University of Technology. Her research interests are lab-on-a-chip technologies and cell chip technologies with focus on sensor-integrated organ-on-a-chip systems for toxicological research as well as biosensor development for molecular diagnostics.

Tomas Buryska received his PhD in Microbiology from Masaryk University in Brno, Czech Republic. During his PhD studies, he developed high throughput characterization tools, combining protein engineering with microfluidics. He obtained substantial knowledge in the field during his many research stays at the University of Cambridge and Technical University Wien. Currently, working as a postdoc at ETH Zurich in the group of Andrew deMello he pursues his career by further developing the tools applicable in biophysics and protein engineering.

Peter Ertl holds a degree in biotechnology (BOKU, Austria), a doctorate in chemistry (Univ. Waterloo, Canada) and postdoctoral training as a biophysicist at the University of California at Berkeley (USA). In addition, Dr. Ertl co-founded a biotech start-up company, where he worked for several years as Director of Product Development at Kitchener-Waterloo (CAD) for the development of cell analyzers in laboratory bench format. In 2005, Dr. Ertl to Austria, where he worked as a Senior Scientist in the BioSensor Technology department at the AIT Austrian Institute of Technology. In 2016 he was appointed professor for lab-on-a-chip systems for life science technologies at the Faculty of Technical Chemistry at the Vienna University of Technology. His research focus is the development of organ-on-a-chip and chip-in-organ systems for biomedical research.

Torsten Mayr received his Ph.D. in chemistry from the University of Regensburg (Germany) in 2004. In 2002–2004 he was a post-doctoral fellow at the KarolinskaInstitute in Stockholm (Sweden). Since 2004 he is assistant professor at the Instituteof Analytical Chemistry and Food Chemistry at the Graz University of Technology. Since 2014 he is Associate Professor the same institute. His research interests includeoptical chemical sensors, biosensors, functionalized micro- and nanoparticles, flow chemistry, lab-on-chip systems, micro-bioreactors and organ-on-chips.